Asian Journal of Chemistry; Vol. 33, No. 11 (2021), 2615-2620
ASIAN JOURNAL OF CHEMISTRY
https://doi.org/10.14233/ajchem.2021.23380

Thermoelectric Power of Silver Telluride Thin Films and its Thermal Conductivity Applications

M. PREM NAWAZ[1], M. PALANIVELU[1], M. KARUNANITHY[2,3], A. AFROOS BANU[1], A. AYESHAMARIAM[3,*] and K. KAVIYARASU[4,5]

[1]Department of Chemistry, Khadir Mohideen College, (Affiliated to Bharathidasan University), Adirampattinam-614701, India
[2]Department of Physics, SKPD Boys Higher Secondary School, Parrys, Chennai-600108, India
[3]Department of Physics, Khadir Mohideen College (Affiliated to Bharathidasan University), Adirampattinam-614701, India
[4]UNESCO-UNISA Africa Chair in Nanosciences/Nanotechnology Laboratories, College of Graduate Studies, University of South Africa (UNISA), Muckleneuk Ridge, P.O. Box 392, Pretoria, South Africa
[5]Nanosciences African Network (NANOAFNET), Materials Research Department (MRD), iThemba LABS-National Research Foundation (NRF), 1 Old Faure Road, 7129, P O Box 722, Somerset West, Western Cape Province, South Africa

*Corresponding author: E-mail: aamariam786@gmail.com

Received: 21 June 2021; *Accepted*:15 July 2021; *Published online*: 20 October 2021; AJC-20538

The hydrothermal technique was used to create straight single crystal silver telluride nanowires with a diameter of around 200 nm and a length of up to micrometers of decades. There has been no template or surfactant used in the process. As-synthesized products are high purity and well-crystallized, confirmed by X-ray diffraction, scanning electron microscopy, X-ray photoelectron spectrum, transmission electron microscopy (TEM), and a high-resolution SAED pattern. Differential scanning calorimetry was used to observe the reversible structural phase shift from the low-temperature monoclinic structure to the high-temperature face-centered cubic structure. Furthermore, the dramatic drop in electrical current in a single nanowire at the phase transition temperature is revealed, paving the way for future research into the manufacturing of one-dimensional nanoscale devices. Silver telluride (Ag_2Te) has large thermoelectric coefficients and it was tested by using resistor graph and calculated the values of it, thermal conductivity and Seebeck coefficient were discussed with respect to the temperature of thin films. Semiconductors were superior thermoelectric material due to higher ratio of electrical and thermal conductivities. Therefore, the AgTe thin films deposited on indium tin oxide (ITO) substrates were employed, thermoelectric power and thermal conductivity measurements, respectively.

Keywords: Thermal evaporation, Silver telluride, Thermal conductivity, Thermoelectric power.

INTRODUCTION

There has been a lot of interest in new forms of nano-devices based on Ag_2Te nanostructures, which are important because they have promising mechanical, electrical, optical, and magnetic characteristics that are distinct from those of polycrystalline bulks [1]. Li *et al.* [2] prepared the straight single crystal silver telluride nanowires with the diameter of about 200 nm and length upto micrometers by the hydrothermal process without any template or any surfactant. By differential scanning calorimetry, the reversible structural phase transition from the low-temperature monoclinic structure to the high-temperature face-centered cubic structure was observed. The electrical properties of individual Ag_2Te nanowires were investigated by the voltammetric technique, wheren I-V curves were clearly non-linear and symmetrical with respect to both axes.

Suchand Sandeep *et al.* [3] prepared tellurium and silver telluride (Ag_2Te) nanowires in solution and investigated their non-linear optical transmission by the open-aperture *z*-scan technique, using nanosecond laser pulses, at the excitation wavelengths of 532 and 1064 nm. The non-linearity had contributions from absorption saturation, excited state absorption and non-linear scattering processes. The non-linear absorption in Ag_2Te nanowires was found to be one order of magnitude higher than that in Te nanowires. Chen *et al.* [4] discussed about the preparation of crystalline silver telluride films by cathodic deposition from DMSO solutions containing 0.1 M $NaNO_3$, 5.0 mM $AgNO_3$ and 3.5-7.0 mM $TeCl_4$. In contrast, Ag_7Te_4 film consists of triangles characteristic of a (111) single crystal with a hexagonal structure in average sizes of about 0.4 m.

The X-ray photoelectron spectra (XPS) indicated that the binding energies deviation of Te_3d in Ag_7Te_4 is less than that in Ag_2Te, which is consistent with the apparent valences of Te in Ag_2Te and Ag_7Te_4.

Jia *et al.* [5] reported that Ag_7Te_4 nanowires were synthesized into porous anodic alumina membranes by DC electrodeposition from aqueous solution. The effects of several electrodeposition parameters on the Ag_7Te_4 nanowire arrays were also discussed [5]. Li *et al.* [6] reported a simple and clean method of producing nanocrystalline silver tellurides (Ag_2Te and Ag_7Te_4) in organic solvent systems by high-intensity ultrasonic irradiation at room temperature. Feng *et al.* [7] fabricated the ultralong single crystal β-Ag_2Te nanowires with the diameter of about 300 nm through a solvothermal route in ethylene glycol system without any template. The detailed topotactic transformation process from particles into single crystal wires was studied.

Prabhune & Fulari [8] uses double exposure holographic interferometry together with simple mathematical interpretation, which allow immediate finding of stress and thickness of thin film whereas. They noticed that the fringe spacing changes with solution concentration as well as time of deposition. Bindi [9] discussed about the crystal structure of impressive, AgTe, a rare silver telluride and investigated by *in situ* X-ray single crystal diffraction methods within the temperature range 298-463 K. AgTe remains orthorhombic, space group *Pmnb* and showed only normal thermal expansion over the entire temperature range. The unit-cell parameters showed a gradual increase with the increase of temperature. Slight adjustments in the geometry of Ag-tetrahedra and in the crystal chemical environment of tellurium atoms occur in a continuous way without abrupt structural changes. Tursucu *et al.* [10] discussed the K shell intensity ratios K_β/K_α for 9 elements in the atomic range $40 \le Z \le 50$ that were determined using a weak ^{133}Ba gamma source at excitation energy of 80.997 keV. Herein, the preparation and characterization of silver telluride nanowires with high purity, straight and well-crystallized and the structural phase transition of the sample is reported. Moreover, the electrical conductivity of individual Ag_2Te nanowires was also studied by the voltammetric technique.

EXPERIMENTAL

Synthesis: In a typical method, 1.0 mmol silver nitrate and 0.5 mmol sodium tellurate were dissolved in 25 mL distilled water with constant stirring followed by the addition of 0.40 mL aqueous hydrazine solution (80%) and 0.4 mL ammonia (25%) rapidly in succession. The mixture was placed into a Teflon-lined autoclave (50 mL), heated to 180 ºC and kept at this temperature for 24 h [11]. Following the hydrothermal treatment, the precipitate was collected and washed with distilled water and ethanol before being dried in air for subsequent deposition on an ITO plate using thermal evaporation. X-ray diffraction/photoelectron spectroscopy (XRD/XPS, X'pert MRDPhilips diffractometer with Cu*K*α (λ = 0.154056 nm/ AXISULTRA XPS, Al K) was used to determine the phase and composition of the products. Scanning/transmission electron microscopy (SEM/TEM, JEOL JSM5600LV/JEOL 2010, JEOL Ltd., Tokyo, Japan) was used to examine the size and morphology of the as-synthesised Ag_2Te nanowires. Under nitrogen environment, a differential scanning calorimeter (DSC851e, Switzerland) was used with a heating rate of 10 ºC min^{-1}. The single nanowire lapped in Au electrode was assembled using the electric field assembly technique. Starting from an equilibrium condition in nitrogen and a heating rate of 10 ºC min^{-1}, the I-V characteristics at room temperature, as well as electrical current fluctuations from 25 ºC to 205 ºC, were measured with a Keithley 4200-SCS system.

RESULTS AND DISCUSSION

XRD analysis: The XRD patterns of the products for the crystal structures and compositions are shown in Fig. 1. The observed diffraction peaks agree with the expected spectrum according to the monoclinic Ag_2Te crystal structure (JCPDS card No: 16-0412) of diffraction planes (241) and (071). The summarized lattice parameter value was reported in Table-1. Therefore, the diffraction peaks at 2θ = 34.5º and 36.28º can be indexed to (403), (314) of Ag_2Te, annealed samples which are well agreement with the standard diffraction data of powder monoclinic Ag_2Te (JCPDS standard file no: 86-1168) [12]. In Fig. 2, DSC data shows a structural phase transition from the low -temperature monoclinic structure (Ag_2Te) to the high-temperature face-centered cubic structure (Ag_2Te). During heating (top section as indicated with an arrow), a sharp valley was observed at 150 and 300 ºC.

XPS analysis: The XPS spectra include a wide-scan XPS spectrum (Fig. 3a) as well as high-resolution XPS (HRXPS) spectra of Ag-3*d* (Fig. 3b) and Te-3*d* (Fig. 3c). Since a little

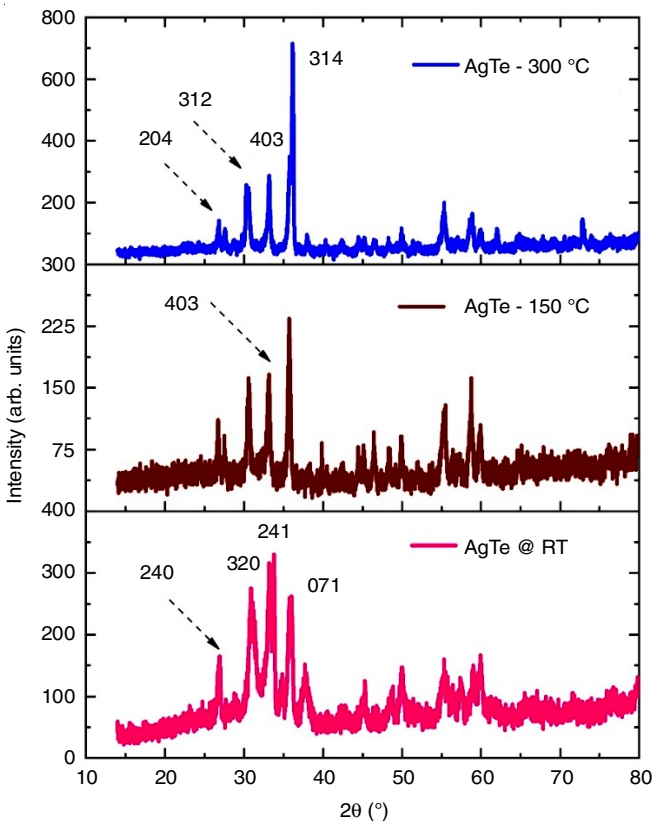

Fig. 1. XRD pattern of Ag_2Te thin film nanostructure at RT, 150 & 300 ºC

TABLE-1
XRD ANALYSIS OF Ag_2Te THIN FILMS

Samples	JCPDS	Crystal size (nm)	Lattice parameter (Å)		
RT	16-0412	42	Orthorhombic α-8.90 (JCPDS) α-8.11	β-20.07 (JCPDS) β-21.01	χ-4.62 (JCPDS) χ-4.19
150 °C	86-1168	51	Hexagonal α-13.45 α-12.99	Nil Nil	χ-16.917 χ-16.32
300 °C	86-1168	59	α-11.59	Nil	χ-16.10

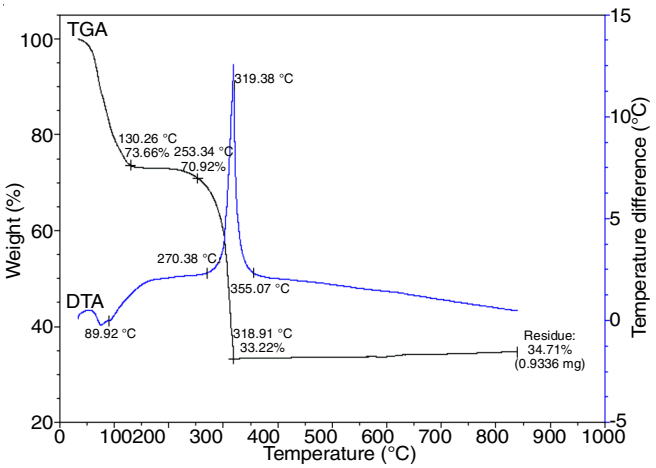

Fig. 2. DSC curve of Ag_2Te thin film nanostructure for 300 ºC

amount of C and O originates from the mechanical pump's lubricant, the as-synthesised products include just Ag and Te components, as shown in Fig. 3a. The peaks at 368.2 and 572.2 eV, respectively, correspond to Ag-3$d^{5/2}$ and Te-3$d^{5/2}$, indicating that the product is made up of Ag^+ and Te^{2+} valence states, according to HRXPS. In addition, two tiny peaks at 576.1 and 586.5 eV, which can be ascribed to Te(IV) oxide, are visible, as shown in Fig. 3c. Furthermore, the molar ratio of Ag to Te, as determined by HRXPS peaks, 1.986:1.00, which is similar to the stoichiometry of Ag_2Te as shown by FTIR spectra (Fig. 4) [8].

For structural analysis, AgTe thin films deposited on ITO substrate were used and there is a slight difference between the phases identified through XRD and EDAX is shown in Fig. 5f and listed in Table-2, which displays the qualitative compositions and the results can be influenced by the surrounding grains and morphological effect as shown in Fig. 5d. All the surfaces were found to be smooth and uniformly distributed with nano grains. The grain size values were found to be about 66, 74 and 85 nm for silver telluride films with tellurium content x = 0.6. It is also reflecting the fact tellurium (high atomic radius) is effective, which leads to larger grained films with (0.6) higher Te content. These proportions of tellurium (0.6) were developed by the presence of alloy structural phases, nanograins and contents of Te [13].

TABLE-2
EDAX ANALYSIS OF Ag_2Te AT ROOM TEMPERATURE

Elements	Net counts	Elements (%)	Atomic (%)
Te	550	5.18	25.35
Ag	1029	3.92	12.62
Ag	412	90.91	62.03
Total	–	100.00	100.00

Thermal conductivity: Nanoparticles increase the heat transfer rate in nanowires by increasing its thermal conductivity and thermal diffusion in flow. Since nanoparticles have much more surface area compared with microparticles and other larger particles and increasing the heat transfer surface area increases the effective surface. This section examines the importance of increasing the percentage of nanoflower compared with an increase in temperature for the purpose of the thermal conductivity improvement [14]. Thermal conductivity of Ag_2Te nanowires with effect of temperature for different weight fractions, thermal conductivity of nanowires, is highly dependent on temperature. Increasing of the temperature leads to increasing of the thermal conductivity of nanowires. One of the reasons which play an important role in temperature dependency is the Brownian motion phenomenon that increases the motion and oscillation of nanoparticles due to temperature rising, so that the viscosity of the base fluid decreases by the temperature rise which increases the nanoparticles garbled motion [15]. The morphology of the nanoparticles used in this study is the rod type, so these rods can act as a heat transfer bridge. Also, the heat transfer coefficient will be increased by rising the percentage of the nanowire (Fig. 6). The percentage increase of heat transfer coefficient based on the weights of nanowire, between room temperature to 300 ºC [16]. The Seebeck coefficient was determined using the formula S = V/T, where V and T were the induced thermoelectric voltage across the materials and the through-plane temperature differential of the films, respectively.

Resistograph method to find thermoelectric power of Ag_2Te: For a thermoelectric material, which must be used in device fabrication the value of Seebeck coefficient should be as high as possible here we reported it varies from 124.5, 126.9 and 129.5 (μV/K) for the film at room temperature, 150 and 300 ºC (Table-3). The resistivity of a given semiconductor may be diminished by addition of controlled amounts of impurities. This doping process affects both carrier concentration and mobility of the charge carriers, resistivity $p = 1/ne\mu$, here n is the concentration of charge carriers, e represents the charge and μ denotes their mobility [17]. Constant current selectable from 1 to 50 mA was passed through the samples, which were

TABLE-3
THERMAL PROPERTIES, SEEBECK COEFFICIENT OF Ag_2Te

AgTe	Seebeck voltage (μV)	Temperature difference (°C)	Seebeck coefficient (μV/K)	Thermal conductivity (mW/Cm K)
RT	41	0.35	124.5	6.9
150 °C	78	0.69	126.9	5.5
300 °C	79	0.71	129.5	5.3

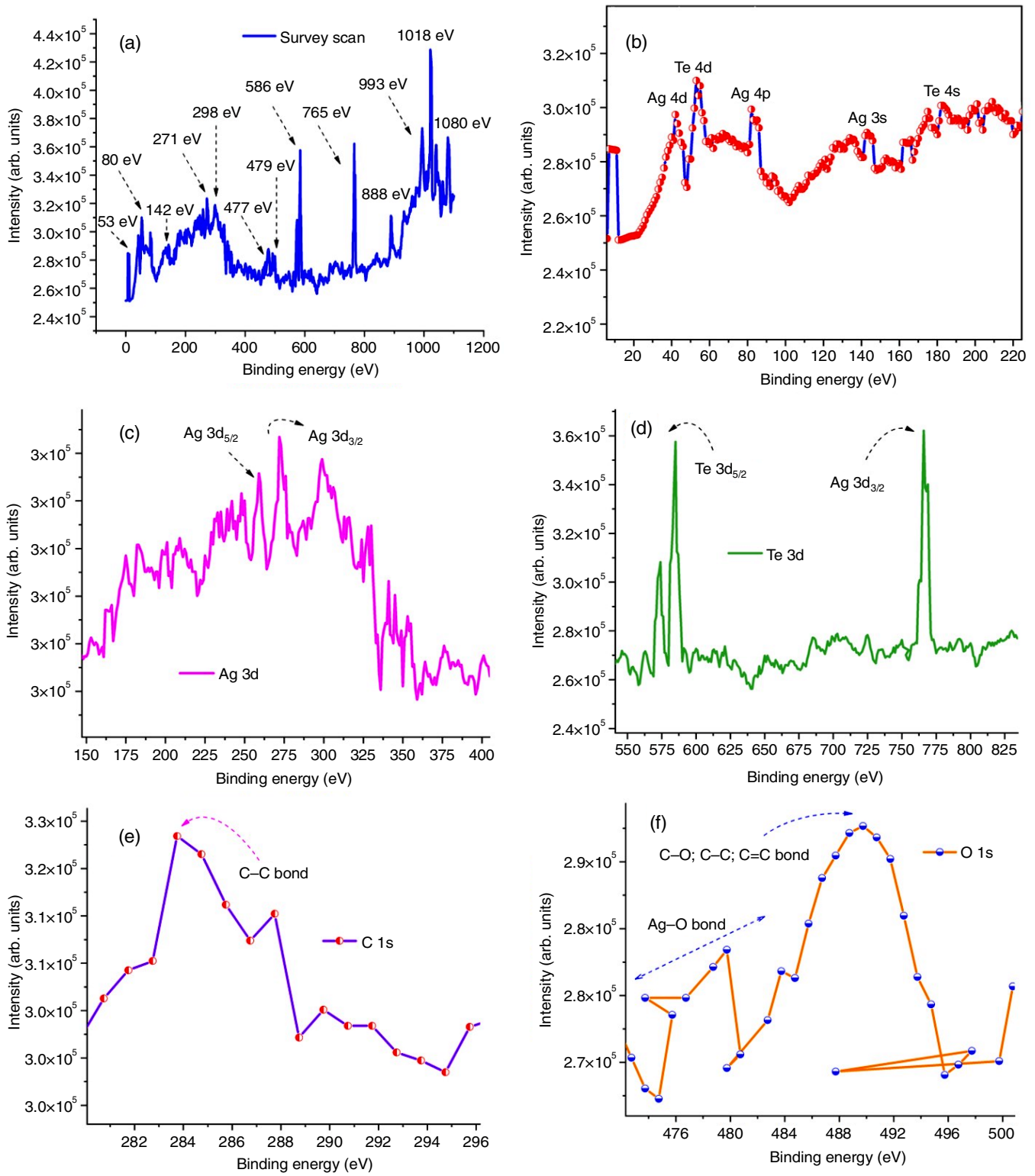

Fig. 3. XPS studies of Ag_2Te thin films nanostructure at room temperature

kept inside the furnace. The voltage developed is measured by the DC (μV) amplifier the temperature of the furnace and in turn the samples temperature was increased by increasing the power fed through the furnace. The data was collected automatically using the PC 24 data acquisition card and stored in the file [18].

When a direct current was used for studying the material processing a high Seebeck coefficient the temperatures at the voltage probes may be different, because of Peltier effect. The non-uniform temperature may result in Seebeck voltage, which is added to the observed potential drop across the samples [19]. The phenomenon can result in large errors in the observed

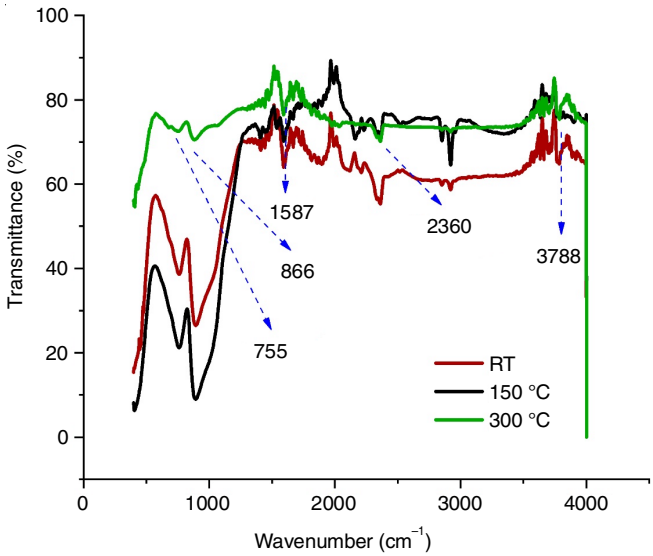

Fig. 4. FTIR spectrum of Ag_2Te nanostructure at RT, 150 °C and 300 °C

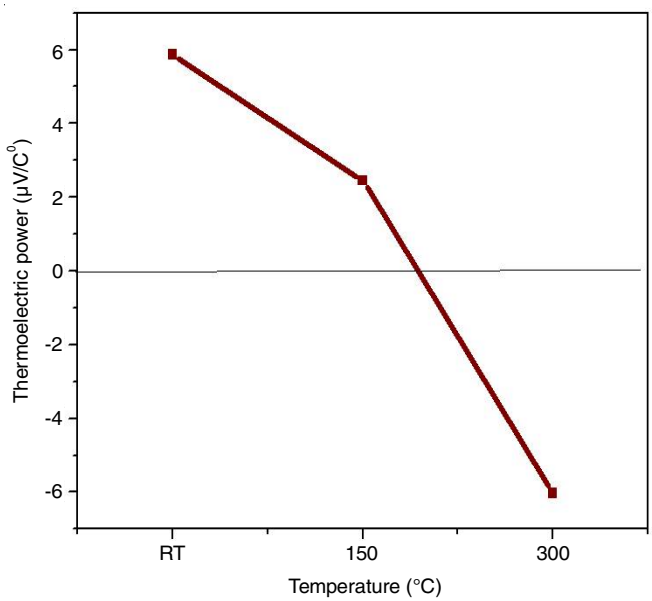

Fig. 6. Thermoelectric power *vs.* temperature of the samples Ag_2Te thin film

resistivity of the three samples (Table-4). When the open circuit voltage is created by the temperature differential between two locations on a wire with a uniform difference of 1K between them, the Seebeck coefficient [21] was used.

TABLE-4
THERMOELECTRIC POWER OF
Ag_2Te AT RT, 150 °C AND 300 °C

Samples	Voltage (mV)	Resistance (ohms)	Resistivity (Ohm cm^{-1})	Thermo power (mV/C)
AgTe (RT)	50.9	5.19	0.0035	5.8693
150 °C	15.4	1.54	0.0012	2.4586
300 °C	9.80	0.98	0.0009	-6.0252

Conclusion

In summary, the solid solutions of silver telluride (Ag_2Te) binary compounds have been deposited on indium tin oxide (ITO) substrates through Thermal evaporation route. The XRD studies showed continuous variation in 'a' value confirming

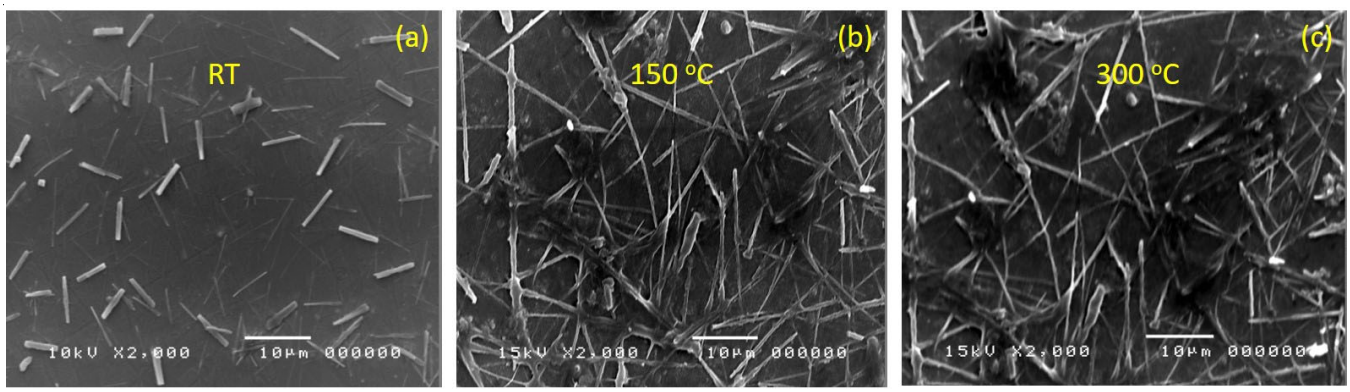

Fig. 5(a-c). SEM analysis of Ag_2Te at RT, 150 ºC and 300 ºC

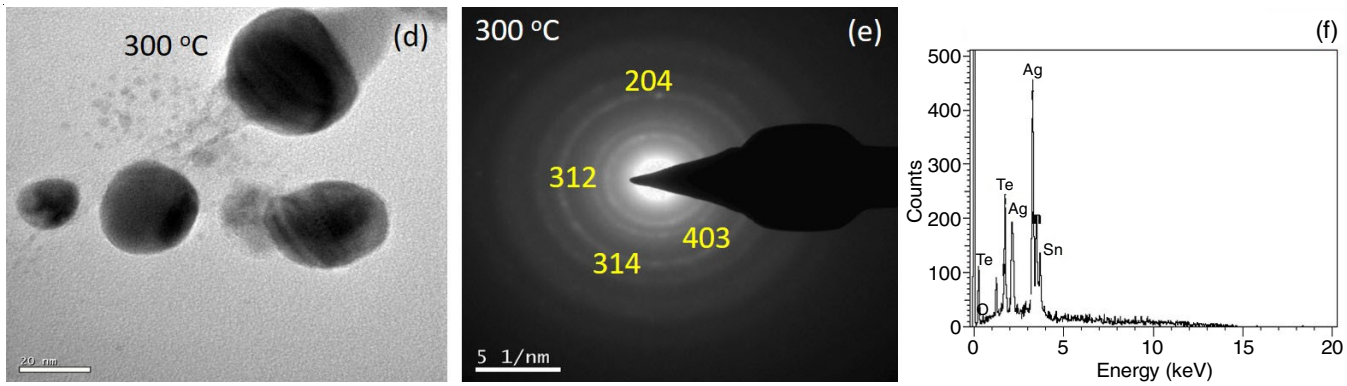

Fig. 5(d-e). TEM and SAED pattern of Ag_2Te and Fig 5(f) EDAX analysis of Ag_2Te at RT

the solid solution formation. Surface morphological studies by SEM and TEM with SAED pattern showed a uniform surface with globular grains. The thermal conductivity values were very high owing to the formation of larger silver vacancies in the crystal lattice. Thermoelectric power was also low and negative for the sample at 300 ºC.

CONFLICT OF INTEREST

The authors declare that there is no conflict of interests regarding the publication of this article.

REFERENCES

1. B. Zhong, X. Wang, Y. Bi, W. Kang and L. Zhang, *New J. Chem.*, **45**, 6100 (2021); https://doi.org/10.1039/D1NJ00687H
2. N. Li, B. Zhao, S. Zhou, S. Lou and Y. Wang, *Mater. Lett.*, **81**, 212 (2012); https://doi.org/10.1016/j.matlet.2012.05.009
3. C.S. Suchand Sandeep, A.K. Samal, T. Pradeep and R. Philip, *Chem. Phys. Lett.*, **485**, 326 (2010); https://doi.org/10.1016/j.cplett.2009.12.065
4. R. Chen, D. Xu, G. Guo and L. Gui, *Electrochim. Acta*, **49**, 2243 (2004); https://doi.org/10.1016/j.electacta.2004.01.004
5. C. Jia, B. Zhang, W. Liu, C. Jin, L. Yao, W. Cai and X. Li, *J. Cryst. Growth*, **285**, 527 (2005); https://doi.org/10.1016/j.jcrysgro.2005.09.007
6. B. Li, Y. Xie, Y. Liu, J. Huang and Y. Qian, *J. Solid State Chem.*, **158**, 260 (2001); https://doi.org/10.1006/jssc.2001.9103
7. J. Feng, J. Zhao, B. Tang, P. Liu and J. Xu, *J. Solid State Chem.*, **183**, 2932 (2010); https://doi.org/10.1016/j.jssc.2010.09.043
8. V.B. Prabhune and V.J. Fulari, *Opt. Commun.*, **282**, 2118 (2009); https://doi.org/10.1016/j.optcom.2009.02.029
9. L. Bindi, *J. Alloys Compd.*, **473**, 262 (2009); https://doi.org/10.1016/j.jallcom.2008.05.043
10. A. Tursucu, P. Onder, E. Eroglu and D. Demir, *Appl. Radiat. Isot.*, **70**, 1509 (2012); https://doi.org/10.1016/j.apradiso.2012.04.029
11. P. Gnanadurai, N. Soundararajan and C.E. Sooriamoorthi, *Phys. Status Solidi*, **237**, 472 (2003); https://doi.org/10.1002/pssb.200301743
12. N.M.I. Alhaji, D. Nathiya, K. Kaviyarasu, A. Ayeshamariam and M. Meshram, *Surf. Interfaces*, **17**, 100375 (2019); https://doi.org/10.1016/j.surfin.2019.100375
13. M. Karunanithy, G. Prabhavathi, A.H. Beevi, B.H. Ibraheem, K. Kaviyarasu, S. Nivetha, N. Punithavelan, A. Ayeshamariam and M. Jayachandran, *J. Nanosci. Nanotechnol.*, **18**, 6680 (2018); https://doi.org/10.1166/jnn.2018.15731
14. P.M. Anwar, S. Muruganantham, M. Karunanithy, M. Benhaliliba, A. Ayeshamariam, M. Jayachandran and K. Kaviyarasu, *Mater. Today Proc.*, **36**, 492 (2020); https://doi.org/10.1016/j.matpr.2020.05.148
15. B. Russ, Doctoral Dissertation, Design Rules for Solution-Processable n-type Organic Thermoelectric Materials, University of California, Berkeley, USA (2015).
16. S.L. Kim, Doctoral Dissertation, Thermally Driven Energy Conversion and Storage Based on Organic Nanocomposites, Texas A & M University, USA (2017).
17. B. Lorenzi, Doctoral Dissertation, Nanocrystalline Silicon as a Thermoelectric Material-Bring the Nanotechnological Advantage into Bulk (2015).
18. I. Petsagkourakis, Doctoral Dissertation, High Performance Polymer and Polymer/Inorganic Thermoelectric Materials, Université de Bordeaux, France (2016).
19. O. Uemura, T. Sekiya, H. Ishikawa and T. Satow, *Ber. Bunsenges. Phys. Chem*, **90**, 71 (1986); https://doi.org/10.1002/bbpc.19860900112
20. M.H. Lee, D.G. Byeon, J.S. Rhyee and B. Ryu, *J. Mater. Chem. A Mater. Energy Sustain.*, **5**, 2235 (2017); https://doi.org/10.1039/C6TA09941F